Physica 23D (1986) 413–435
North-Holland, Amsterdam

ROBUST SPACE-TIME INTERMITTENCY AND 1/f NOISE

James D. KEELER
Physics Department and Institute for Nonlinear Science B-019, University of California, San Diego, La Jolla, CA 92093, USA

and

J. Doyne FARMER
Center for Nonlinear Studies, MS B258, Los Alamos National Laboratory, Los Alamos, NM 87545, USA

We investigate a type of intermittency that occurs in space as well as time, studying a one dimensional lattice of coupled quadratic maps. This system naturally forms spatial domains. Motion of the domain walls causes spatially localized changes from chaotic to almost periodic behavior. The almost periodic phases have eigenvalues quite close to one, resulting in long-lived laminar bursts with a $1/f$ low frequency spectrum. This behavior has aspects of both Crutchfield and Pomeau–Manneville intermittency. Unlike Pomeau–Manneville, however, the behavior that we observe here is quite robust under changes of parameters.

1. Introduction

Space–time intermittency is one of the most baffling phenomena observed in spatially extended systems. A common manifestation occurs in fluid flows, where patches of turbulence are sometimes isolated in space. The interface between laminar and turbulent behavior is dynamic and, at least to the casual observer, unpredictable; without changing parameters, turbulence can spread through the entire flow, or dissapear, so that the entire flow becomes laminar. A good example are the turbulent spots seen in doubly rotating Taylor–Couette flow [1]. In general, space-time intermittency occurs whenever two qualitatively different types of behavior are intermittent in both space and time.

To our knowledge there are no theories for space–time intermittency, even though it is observed in many physical systems. Our approach to this problem is to study the simplest possible example, in this case a one dimensional lattice of coupled quadratic maps, as studied by Crutchfield [2], Diessler [3], Kaneko [4, 5], and Waller and Kapral [6]. This system displays space–time intermittency through a wide range of parameter values. An example is shown in fig. 1.

Before describing our results, we would like to make a few remarks about our approach. Recent developments in the study of low dimensional dynamics have shown the efficacy of obtaining qualitative results through the study of maps rather than flows. Many important physical phenomena such as the discovery of the U-sequence [7], period-doubling [8], etc., were originally discovered in low dimensional maps and later observed in experiments. Low dimensional maps are not sufficient, however, to describe phenomena that are intrinsically spatial.

Physical models with spatial degrees of freedom tend to be written down either as partial differential equations or continuous-time lattice models. Such models are difficult to study, both numerically and analytically. Through the method of Poincaré section, however, partial differential equations can always be reduced to iterated functional mappings, continuous in space but discrete in time. Thus every partial differential equation

0167-2789/86/$03.50

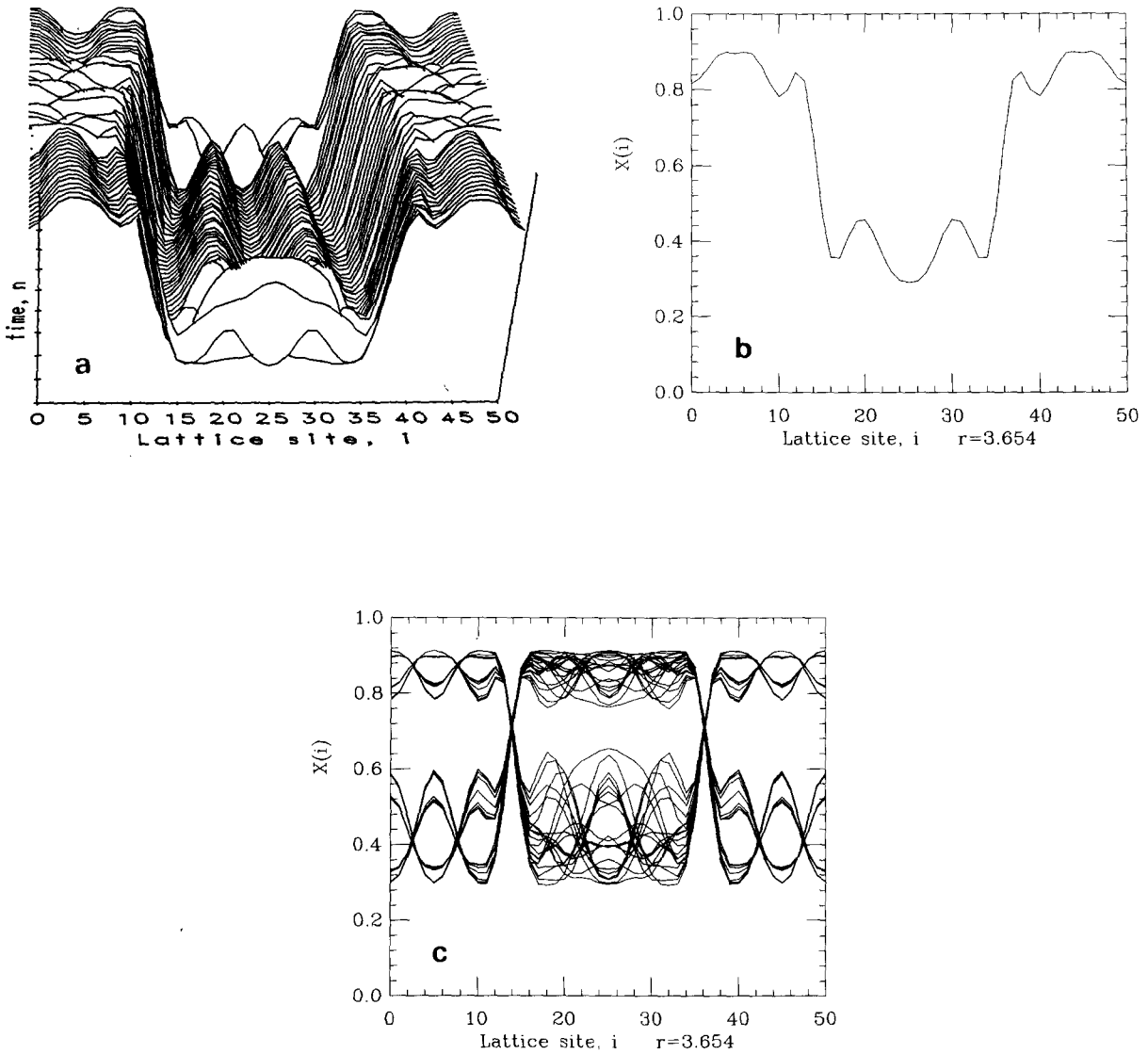

Fig. 1. (a) A perspective view of time evolution of eq. (4) with $r = 3.654$ and $a = 18\frac{2}{3}$. Time increases from front to back and the lattice is arranged from left to right. The vertical dimension represents the value of the solution. Lines were drawn between each point on the lattice to approximate a continuous function by linear interpolation. Due to the periodicity of the laminar phases, only every 32nd iteration is shown. The laminar regions look smooth, in contrast to the chaotic regions. At any given time the lattice may be entirely chaotic, entirely laminar, or contain a mixture of chaotic and laminar phases. (b) The configuration of the lattice at a given instant in time; for this snapshot one domain is chaotic while the other is laminar. (c) Several configurations of the lattice plotted simultaneously, illustrating the difference between laminar and chaotic behavior. (d) The time series produced at a fixed lattice position.

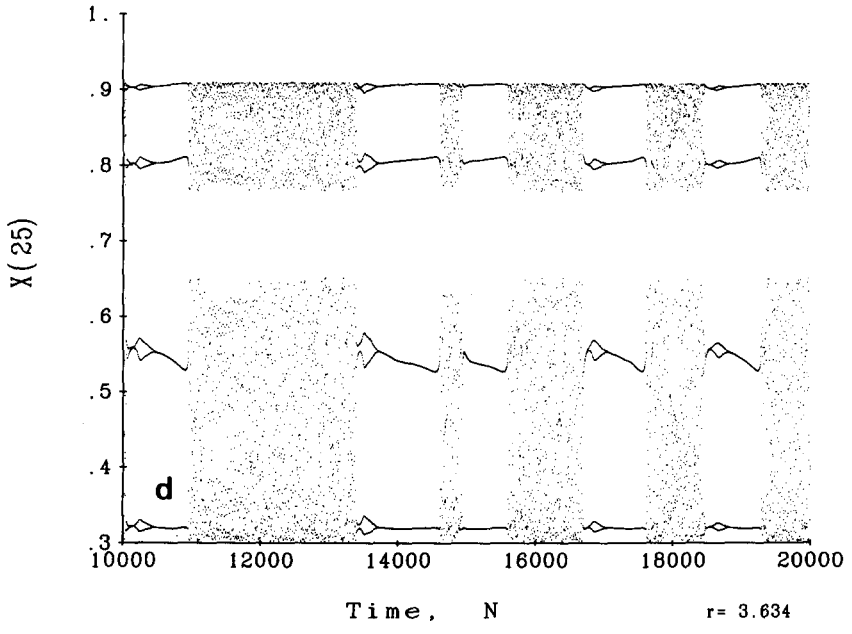

Fig. 1. continued.

has an infinite set of equivalent iterated functional mappings, even though it may be difficult if not impossible to explicitly write any of them down. We reverse this procedure, explicitly writing down a functional map that is easy to study, knowing that there are classes of partial differential equations corresponding to it. In fact, the functional map that we study here is the type expected from a reduction of a driven reaction–diffusion equation [9]. To simplify things still further, we use a discrete spatial lattice, reducing the functional map to a lattice map. As the simplest systems with spatial degrees of freedom, lattice maps provide a natural environment for the qualitative study of dynamics in higher dimensions.

2. A brief review of previous theories of intermittency

There is very little literature on space–time intermittency. What is known tends to be very heuristic. For example, a variety of space–time intermittency occurs in turbulent wakes: Often there is a fluctuating interface between turbulent and laminar flow, which is quite well defined. If a probe is placed in fixed point in space in the region of the wake, the resulting time series shows sharp transitions between turbulent and laminar behavior. This is quite different, however, from space–time intermittency that we discuss here, which has more complicated spatial behavior. We know of no previous theories for the variety of space–time intermittency studied here.

There are three known types of temporal intermittency, described by Pomeau and Manneville [10], Grebogi et al. [11], and Crutchfield [12]. We present a brief review.

A major step in the understanding of temporal intermittency was made by Pomeau and Manneville [10]. The basic idea is quite simple: When a periodic cycle becomes unstable, by continuity there is a region in parameter space near the bifurcation point where the magnitude of the instability remains small. Orbits near the cycle remain so for some time, during which the motion is nearly periodic. If the cycle is embedded in a chaotic attractor, at irregular intervals trajectories

passes near the cycle, causing sporadic bursts of nearly periodic behavior.

The resulting intermittent behavior can be classified according to the nature of the bifurcation which causes it. There are three basic types:

1) The largest eigenvalue exists through 1.

2) A complex conjugate pair of eigenvalues crosses the unit circle.

3) The largest eigenvalue exists through through -1.

Pomeau–Manneville intermittency occurs only near bifurcations, typically in narrow parameter windows. In addition, there is no explanation of how intermittency might occur in space as well.

Kaneko [5] has shown that Pomeau–Manneville intermittency can turn into space–time intermittency in systems that are spatially extended, providing the spatial coupling is not too large. This behavior exists in only a narrow range of parameters, and is substantially different from what we study here.

Crisis intermittency, originally described by Grebogi et al. [11], occurs when a dynamical system has multiple basins of attractions. For a system with two attractors, for example, it sometimes happens that the basin boundaries of each attractor approaches the other attractor, so that a small noise fluctuation can knock the orbit from one attractor to the other. Like Pomeau–Manneville intermittency, this occurs only in narrow parameter windows, and there is no explanation of how this might occur in space as well.

A very different type of intermittency was proposed by Crutchfield [12]. To understand his idea, consider a dynamical system whose degrees of freedom can be decomposed into fast variables x, and slow variables s, in the following form:

$$\dot{x} = F(x, s), \tag{1a}$$

$$\dot{s} = S(s). \tag{1b}$$

If s is sufficiently slow it can be viewed as a control parameter of the fast system. Suppose that the fast system has a bifurcation from periodic to chaotic behavior on a critical surface s_c. If s is chaotic and crosses through s_c, x will exhibit bursts of chaotic and periodic behavior. This is not restricted to bifurcation points, and can occur through a wide range of parameters.

It is fairly easy to construct examples of Crutchfield intermittency by hand, using familiar systems with the appropriate properties, e.g., two Rossler systems with different time scales. It would be much more convincing, however, to find such behavior in a more natural context. The system we study here provides just such a context. Slow scale variables emerge spontaneouslly from the interactions between the faster scale variables. Since these variables change in space as well as time, the resulting bifurcations are localized in space. As we shall show, the "laminar" behavior corresponds to nearly stable cycles, so in this sense our model for intermittency combines elements of both Crutchfield and Pomeau–Manneville intermittency.

3. Description of the quadratic map lattice

The system we study here consists of a lattice of N quadratic maps coupled together by taking a simple weighted average of each lattice point with its neighbors. That is, at each point we apply the map f and then average over A adjacent positions. More precisely,

$$x_{t+1}(i) = \sum_{j=i-A}^{i+A} f(x_t(j))w(i, j)), \qquad i = 0, 1, 2, \ldots, N, \tag{2}$$

where the integer t indicates the time step, $x(i)$ is the value at the ith lattice site, and $w(i, j)$ is a weighting function. In all of the results reported here f is the logistic map, i.e.

$$f(x) = rx(1 - x). \tag{3}$$

We generally study periodic boundary conditions, $x(0) \equiv x(N)$, but at times we also use fixed boundary conditions as a diagnostic tool.

As mentioned above, this system corresponds to a reaction–diffusion equation. The averaging process supplies the diffusion, and the iteration of the logistic map supplies the reaction. In fact, as $N \to \infty$, for a Gaussian weighting function eq. (2) is equivalent to

$$\frac{\partial x}{\partial t} = \alpha^2 x_{yy} + [f(x) - x]G(t),$$

where $G(t) = \sum_{n=1}^{\infty} \delta(t-n)$, and α is the diffusion constant. The quadratic form of f is somewhat arbitrary. We have also tried other types of maps, including a sin map and an exponential map. Providing the map has a single maximum, the results we obtain are qualitatively similar. For convenience, though, all the results presented here are for the logistic map.

Our numerical experience shows that the qualitative behavior is not very sensitive to the precise form of the weighting function, provided the effective diffusion length is kept constant. For convenience, then, for the remainder of this study we take w to be a boxcar function, i.e., $w(i, j) = 1/(2A + 1)$ for $|i-j| < A$, and $w(i, j) = 0$ for $|i-j| > A$. Equation (2) then takes the simple form

$$x_{t+1}(i) = \frac{1}{2A+1} \sum_{j=i-A}^{j=i+A} f(x_t(j))). \tag{4}$$

This system has three parameters, r, A, and N. r plays the role of a forcing parameter, and A determines the effective diffusion rate. Most of our calculations were done with $A = 1$ and $N = 50$, although many of them were checked with $A = 2$ and $N = 100$. Providing N/A is held constant we find that the qualitative behavior is unchanged by varying N, providing roughly $N > 30$. Varying this ratio has much the same effect as varying the aspect in other spatial systems, and by analogy we call $a = N/(2A + 1)$ the *aspect ratio.*

Although all of our simulations are done on a finite lattice, we often make use of the continuum limit in the discussion. Letting y represent the continuous lattice variable, the diffusion operator that we are using can be written as

$$D_y(x) = \frac{1}{2A} \int_{y-A}^{y+A} x(\hat{y})\, \mathrm{d}\hat{y} \tag{5}$$

and the lattice mapping becomes

$$x_{t+1}(y) = D_y(f(x_t)). \tag{6}$$

The behavior of eq. (2) is quite rich. In spite of the complexity of phenomena there are, however, certain organizing principles that make the behavior of this system more comprehensible. Before giving an overview of the phenomenology, we discuss two important properties of the system, namely kinks and the existence of a natural wavelength.

4. Kinks and spatial domains

One of the interesting properties of this system is that it spontaneously organizes itself into domains, spatial structures that are reminiscent of solitons. This comes about due to the formation of kinks, i.e., regions in which the lattice makes sharp upward transitions, and *antikinks*, regions in which the lattice makes sharp downward transitions, as shown in fig. 2. As seen in fig. 2(a), kinks and antikinks are naturally paired, together forming *domain walls* that divide the lattice into *domains*. Coupling between points inside the same domain is strong, but coupling between points in different domains is weak. These domains play an important role in organizing the space time behavior of the system.

For $r < 3$ kinks are not allowed, due to the fact that the uncoupled logistic map has a unique stable fixed point. Even when coupling is added, the flattening effect of the diffusion on the lattice combines with the tendency of the individual maps to move the solution toward the fixed point, so that regardless of initial conditions the lattice asymptotically approaches a unique flat solution.

As r is increased past 3 the system period doubles. As a result, nonuniform initial conditions

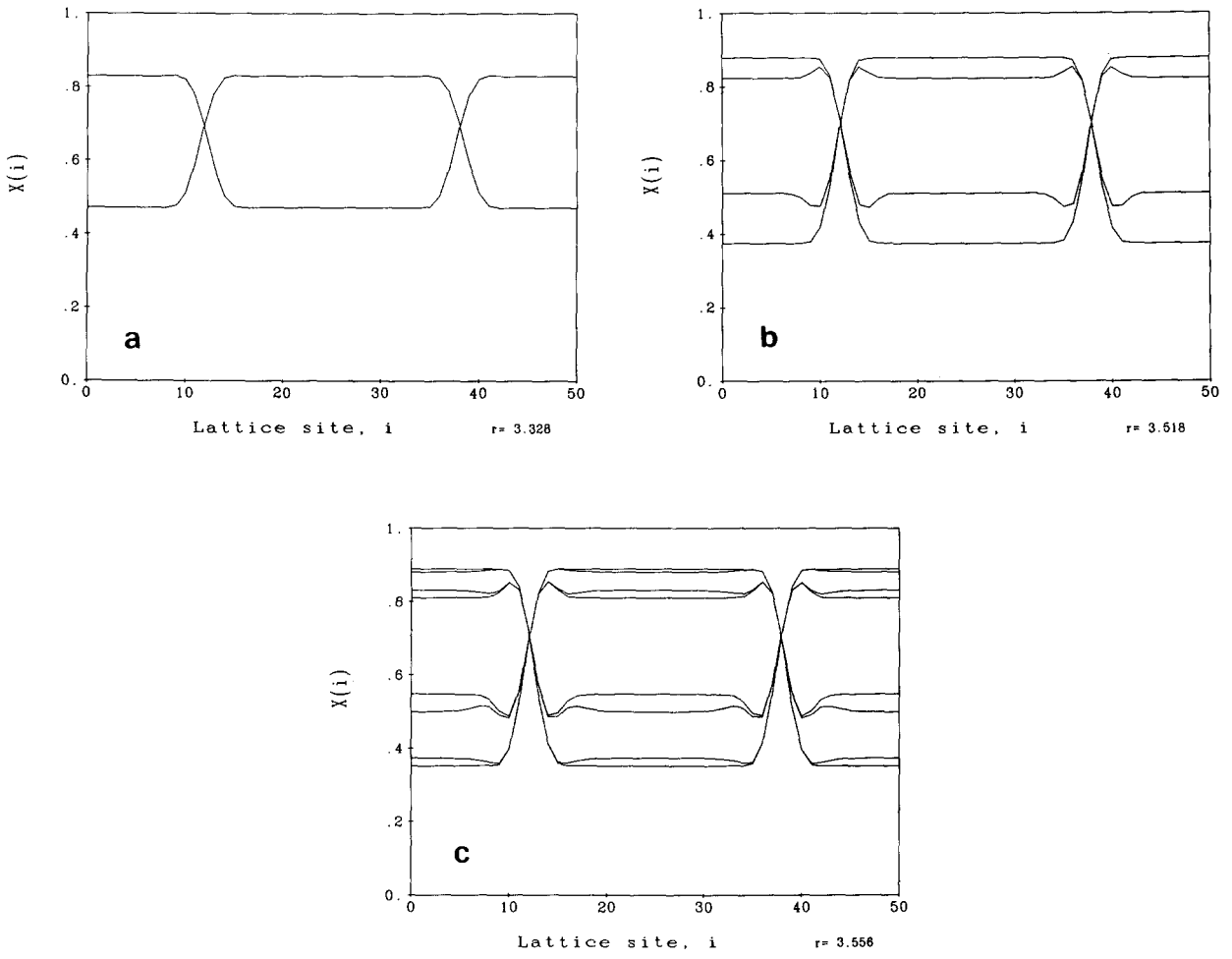

Fig. 2. A typical period doubling sequence. The configuration of the lattice is shown at 40 successive iterations, once transients have died away. In every case $a = 18\frac{2}{3}$, and the initial condition was chosen to generate two spatial domains. (a) $r = 3.328$: A period 2 solution, as seen from the fact that there are only two distinct lattice configurations. The kink–antikink pair forms a domain wall, while the straight sections in between form domains. (b) $r = 3.518$: A period 4 solution. (c) $r = 3.556$: A period 8 solution.

can generate kinks, as illustrated in fig. 2. To understand why this happens, first consider the case of no coupling ($A = 0$), in which each individual map behaves independently of its neighbors. Although the period two cycle of each individual map has a unique basin of attraction, different initial conditions can asymptotically approach solutions of different phase. In other words, if the stable two cycle consists of x_1 and x_2, some orbits asymptotically approach $x_1, x_2, x_1, \ldots$ while others approach $x_2, x_1, x_2, \ldots$. When the initial configuration of the lattice is nonuniformm, different sections of the lattice chose different phases, so that at any given iteration, one section may lie close to x_1, while another lies close to x_2, generating a discontinuity or "kink" in the lattice.

With coupling the kinks persist, except that they are somewhat smoothed out and may extend over several lattice sites. With circular boundary conditions continuity requires that the number of kinks equal the number of antikinks. On each iteration the flat sections of the lattice trade places, causing

a temporal oscillation of period 2. The kinks trade place with antikinks, but there is a special point in the center which remains roughly stationary, which we call a *node*. Typically nodes do not lie precisely on lattice sites, but since the system has a continuum limit this is not a problem.

Mobility of the domains depends on the nature of the coupling. For stable periodic motion the kinks and hence the domains are completely stationary. For chaotic motion the kinks can move, although since the lattice map studied here has symmetric coupling, there is no overall dynamical bias, and the long term average of the movement is zero. Nonetheless, the local movement of the kinks plays an important role in space–time intermittency.

Whether or not the number of kinks and hence the number of domains is conserved depends on parameter values, and is in general related to temporal periodicity properties. A problem in this is that the notion of a kink is not always well defined. We define a "kink" as any region in which $x(i)$ makes a significant and sharp change. For examples such as those of fig. 2, this is clear, but for an arbitrary initial condition, it may be very difficult to predict what will generate a kink and what will not.

Consideration of the uncoupled case makes this clearer. Assume, for example, that r is picked so that the simple one dimensional map has a stable period 2 solution. Consider an arbitrary initial condition, which may or may not have features that obviously give rise to kinks. After iterating for a while some of the individual maps will settle into one phase of the orbit, while others settle into the opposite phase. After transients have died out sufficiently the lattice will consist of flat sections separated by discontinuities. The notion of kinks is now clear and the total number of kinks is conserved for subsequent times. Because the phase basins of the $f(x)$ are in general quite complicated [13] the initial condition may offer few clues about the final configuration of kinks. The definition might be extended to an arbitrary initial condition by defining a kink in terms of basins of attraction, but this would not carry over to the coupled case. Nonetheless, even with coupling, it is intuitively clear that once the solution gets sufficiently close to a stable cycle the number of kinks is conserved.

The number of kinks can also be conserved when the behavior is chaotic, providing the underlying behavior of the uncoupled maps is semiperiodic [14, 15]. To review briefly, for low dimensional strange attractors there are often parameter regions where chaotic behavior is confined to narrow strips or "bands". On successive iterations the orbit cycles between these bands periodically, even though motion within each band is chaotic. The result is chaos that nevertheless has a rough periodicity, dubbed *semi-periodicity* by Lorenz [14].

To understand how this effects conservation of kinks, begin by considering an uncoupled lattice. For simplicity, assume that the individual maps are semiperiodic with period 2. Choose an initial condition so that one section of the lattice is trapped inside in the right band, while a neighboring section is trapped in the left. Since the phase difference between the two sections of the lattice is preserved, the kink that joins them is automatically conserved. With coupling the situation is much the same, although the kinks are not as sharp and can spread over several lattice sites. Once the band ceases to exist, however, this constraint is relaxed to that new kinks can form and old kinks can annihilate.

5. The natural spatial wavelength

Another aspect of this system that plays an important role in space–time intermittecy is the existence of a stable natural spatial wavelength. This comes about through the competition between reaction and diffusion: Chaos tends to buckle the lattice, while diffusion tends to smooth it. At the proper spatial wavelength these effects balance and the lattice is more stable than it is at any other wavelength. Even when the motion is

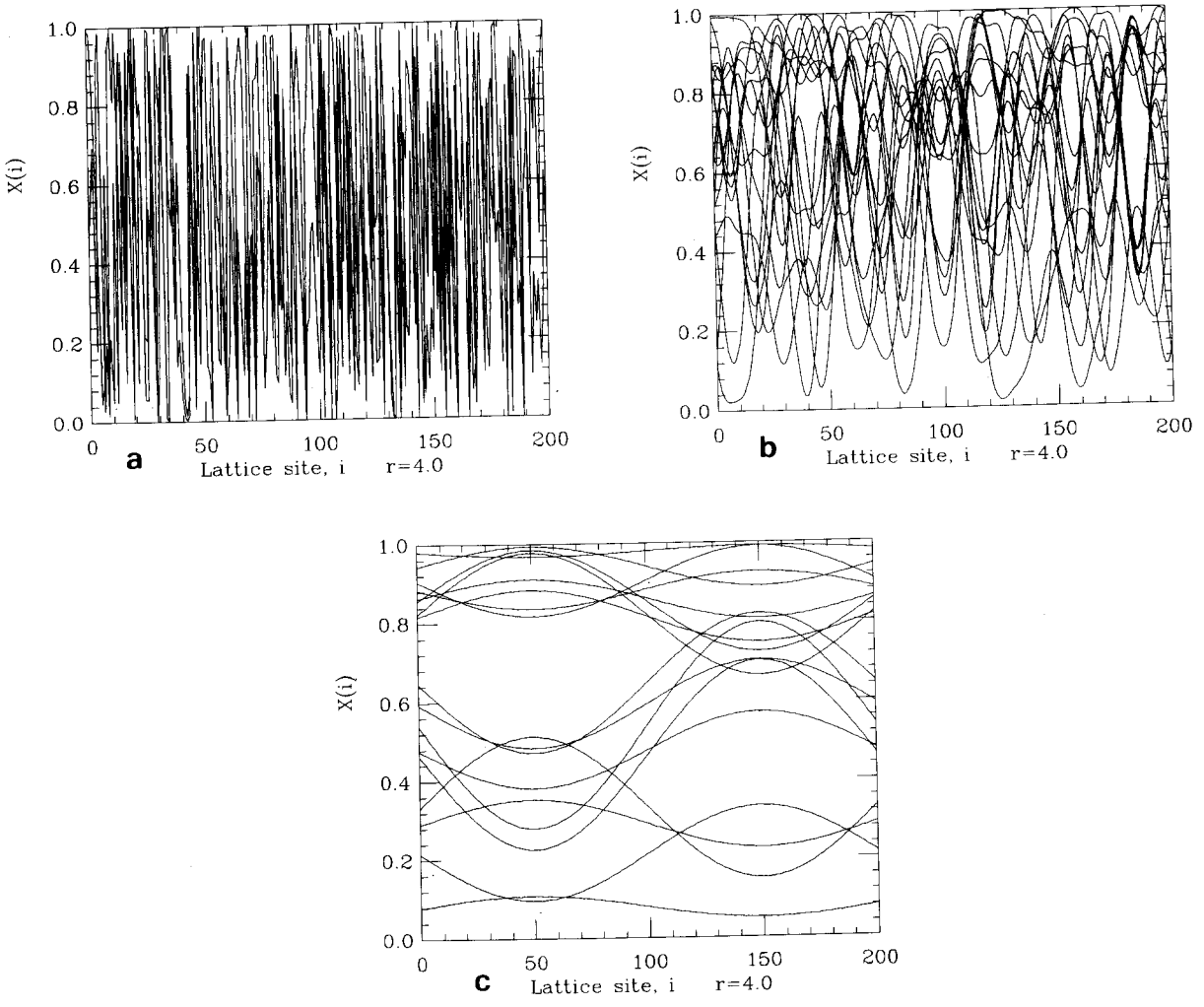

Fig. 3. An illustration of the change in behavior as the diffusion parameter is increased (equivalent to decreasing the aspect ratio). In each case we show a typical lattice configuration at $r = 4$. (a) $a = 50$; (b) $a = 18.2$; (c) $a = 2$.

chaotic this remains the characteristic wavelength of spatial oscillations.

The natural wavelength varies with aspect ratio more or less as you might expect. As the diffusion is increased the lattice gets smoother. This is clearly seen in fig. 3. r is held fixed at 4, and the aspect ratio is varied by changing A. For $a = N$ ($A = 0$) each logistic map behaves independently and the spatial variations are random with a white spectrum. As the diffusion increases the spatial variations become more gradual, so that the central frequency in the spectrum goes down. Finally, if the aspect ratio is on the order of 1 the diffusion dominates and the solution is flat. The dimension d behaves in a corresponding manner: Assuming the individual maps are chaotic, for $a = N$, $d = N$; for $a = 1$, $d = 1$; otherwise d is somewhere between these two values.

The natural wavelength can be crudely estimated as follows: In the continuum limit (in space), let $x_t(y)$ be the solution at position y and time step t. Providing the slope of f is greater than one, iteration amplifies spatial variations, i.e., it tends to steepen the lattice by increasing $x'(y)$

$= \partial x/\partial y$. Diffusion, in contrast, tends to flatten the lattice, countering this process. In steady state these two effects balance on average, i.e., $|x'_{t+1}| \approx |x'_t|$. Differentiating eq. (6) and applying the chain rule, gives*

$$x'_{t+1} = f'(x_t) D'_y(x_t). \tag{7}$$

(Here prime denotes differentiation with respect to the argument.) Expanding the integrand in eq. (5) to second order using Taylor's theorem and integrating yields:

$$D_y(x) = x(y) + \frac{A^2}{6} x''(y). \tag{8}$$

Differentiating (8) with respect to y and setting $x'_{t+1} = -x'_t$ (since the map is orientation reversing) yields the following differential equation:

$$\frac{A^2}{6} x''' + \left(1 + \frac{1}{f'}\right) x' = 0. \tag{9}$$

If f' is taken as constant, this has a solution of the form $\sin(2\pi y/\lambda)$ where the wavelength

$$\lambda = \frac{2\pi A}{\sqrt{6(1 + 1/f')}}.$$

In fact f' is not constant, but noting from our numerical experiments that the solution exists roughly in the range $0.4 < x < 0.9$, f' is almost always negative. As a crude approximation the average value of f' in this range is $-\langle |f'| \rangle$. For $r = 4$, $\langle |f'| \rangle = 2$, the Lyapunov number. The wavelength is roughly

$$\lambda \frac{2\pi}{\sqrt{3}} A, \tag{10}$$

*For convenience we have interchanged the order of the reaction f and the diffusion operator D. This can be thought of as shifting the point at which we observe the dynamics by half an iteration. It makes a small difference in the properties, which is negligible here since we are only making a rough estimate anyway.

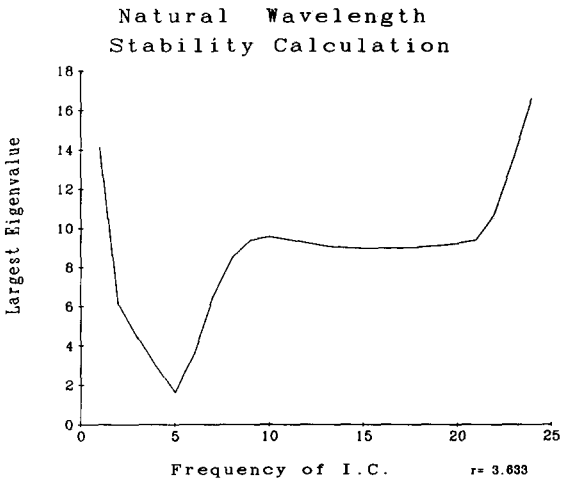

Fig. 4. The largest eigenvalue of the Jacobian matrix for a spatially sinusoidal lattice configuration, as a function of the spatial frequency of the initial condition. The minimum is at roughly the natural wavelength.

which is within a factor of 2 of the true value. This result demonstrates that the natural wavelength depends linearly on the strength of the diffusion.

The natural wavelength can also be estimated in a different way: Given a lattice configuration with a given wavenumber k, of the form

$$x_0(i) = a_0 + a_1 \sin\left(2\pi \frac{ki}{N}\right), \tag{11}$$

we linearize the solution and compute the largest eigenvalue of the Jacobian matrix. When this is plotted as a function of k it has a sharp minimum which corresponds to the natural wavelength, as seen in fig. 4. This estimate agrees quite well with the true value.

The natural frequency plays an important role in space–time intermittency. Before discussing this, however, we must first discuss other important aspects of the phenomenology.

6. Overview of phenomenology

The phenomenology of the lattice map is complicated, and a complete picture is beyond the

scope of this paper. We present only a few salient features here, stressing aspects that are relevant to space–time intermittency. For a discussion of other aspects see Crutchfield and Kaneko [16].

As already mentioned, for $r < 3$ this system has a unique attracting fixed point with a flat lattice. At $r = 3$ the logistic map period doubles, so that for $r > 3$ the lattice admits kinks. This complicates the dynamics considerably, since conservation of kinks implies that a lattice with a given number of kinks cannot approach an attractor with a different number of kinks. The result is a proliferation of attractors, one for each kink number. The number is not infinite, however, since due to the effect of diffusion there is a high frequency spatial cutoff above which kinks are damped so fast that they cannot persist.

Following along as r is increased, intuition based on low dimensional systems suggests that further period doublings should occur. Whether or not this happens, however, depends strongly on spatial properties. For example, consider $a \approx 20$. At one extreme, if the lattice is initially flat, it remains so and behaves like a single map, with a complete period doubling sequence accumulating at the usual value $r = 3.59\ldots$. At the other extreme, if the initial condition has the appropriate number of kinks, it approaches a cycle of period 2, 4 or 8 whose spatial oscillations are near the natural wavelength. These cycles are stable through a wide range of r values. An example is given in fig. 5. For $a = 18\frac{2}{3}$, for example, the cycle shown in fig. 5 is stable for $3 < r < 3.92$.

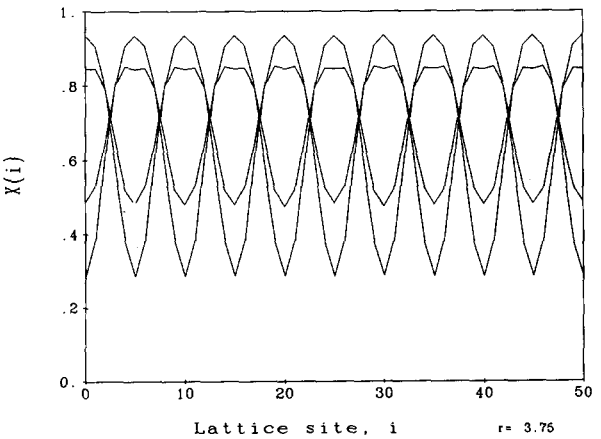

Fig. 5. A cycle whose spatial frequency is near the natural wavelength, stable in the range $3 < r < 3.92$.

Other types of initial conditions give behavior that is intermediate between these two extremes. As r is increased there are typically period doublings, although except for the flat solution they never reach the accumulation point, due to the intervention of a second order spatial oscillation at roughly the natural wavelength. A typical example of this spatial oscillation is shown in fig. 6. As r is raised still further, this oscillation induces its own transition to chaos, pre-empting the period doubling transition. At $a \approx 20$, for example, for two domains the period doubling sequence continues to period 16, at which point the spatial oscillation intervenes. The period 16 orbit gives way to chaos confined in bands of period 16, which then undergo a reverse cascade*. Increasing a tends to reduce the number of period doublings, as does changing the number of domains to be commensurate with the natural wavelength.

As we have seen, the parameter value where the onset of chaos takes place depends on several factors. This complication aside, however, the chaotic regime can roughly be divided into three regions:

Region I

($3.59 < r < 3.7$) *Space time intermittency or stable periodic motion.* (depending on initial conditions).

Region II

($3.7 < r < 3.92$) *Stable periodic motion with possible long lived transients.*

Region III

($3.92 < r < 4$) *Fully chaotic motion.*

(Where it makes a difference, the quoted values

*In this case there are different sizes of kinks, corresponding to the possible transitions between the bands.

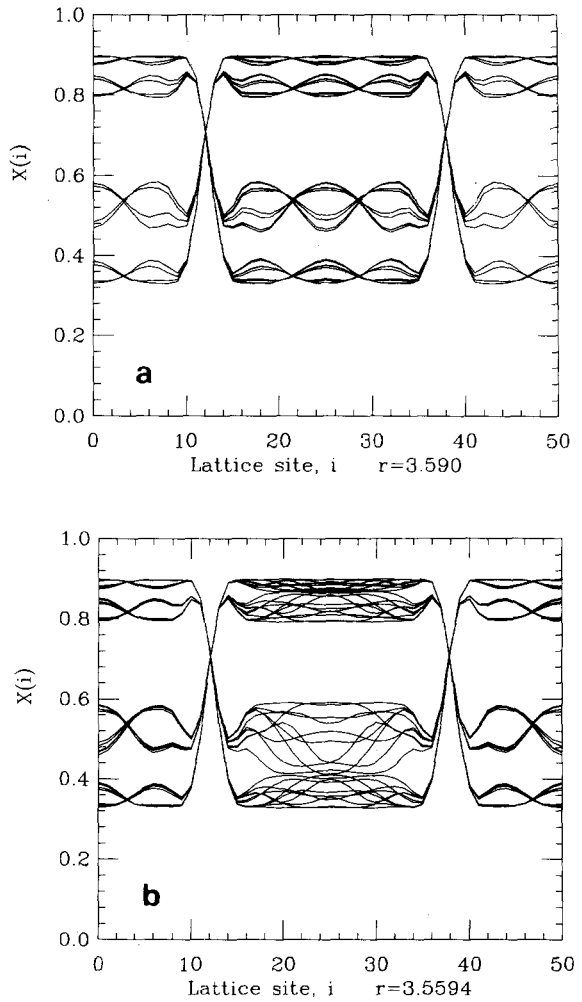

Fig. 6. As r is increased past 3.594 the period doubling sequence is interrupted by a spatial oscillation, at the natural wavelength of the system. This oscillation stabilizes the system, truncating the period doubling sequence and then eventually causing a chaotic transition of its own. (a) A periodic attractor prior to the transition to chaos; (b) chaos after the transition.

are for $a \approx 20$ and spatial solutions with two domains.)

The strong dependence on initial conditions in Region I is largely due to conservation of kinks. Although there are several stable cycles around the natural wavelength, initial conditions that do not have the proper number of kinks are prevented from reaching them. Instead, there is spatial intermittency, as shown in fig. 1.

Region II is defined by the breakdown of kink conservation. Kinks annihilate against antikinks or create new kink–antikink pairs, allowing the number of kinks to adjust until the solution approaches a stable cycle near the natural wavelength.

The parameter value at which kink conservation ceases to occur is highly uncertain. First, there is dependence on initial conditions; the parameter value at which a given number of domains can gain or lose a kink may be different from that for a different number. For example, a transition from four to five domains may become possible at a different parameter value than a transition from five to six. A further complication is strong metastable behavior. This can be understood from the nature of the semiperiodic bands in low dimensional systems; when the bands that generate semiperiodic behavior merge, they do so in a continuous way; near breakdown there is still considerable overlap in the bands, which means that the phase is still approximately conserved and band desynchronization is still rare. The result is that there is a parameter band near the breakdown of kink conservation where kinks are nearly conserved, which generates strong metastable chaos that persists for large numbers of iterations, making it difficult to pinpoint the transition.

The behavior of the uncoupled map provides a guideline for estimating the transition point. The period 2 band which ceases to exist at roughly $r = 3.685$, dominates the behavior we discuss here. For the uncoupled lattice this is the value at which kink conservation ceases. Dissipative coupling resists the formation of new kinks. Most of the initial conditions that we consider have fewer domains than a cycle near the natural wavelength, so that the lattice must add kinks to approach a stable state. For these cases the breakdown of kink conservation is shifted to a larger value of r. Numerically we saw kink conservation until roughly $r = 3.7$. Initial conditions with more kinks, in contrast, must shed kinks to approach a stable state; coupling makes this easier, so that for these cases the breakdown of kink conservation comes

at a lower value of r. The net result is that the boundary between Regions I and II is difficult to define precisely.

Finally, Region III is defined by the parameter value at which all the cycles near the natural wavelength go unstable, giving way to chaos. In this region the number of kinks is variable and there is no space–time intermittency. There is a small band of crisis intermittency near $r = 3.92$, but this occurs only in a very narrow parameter window, in contrast to the phenomenon of interest here.

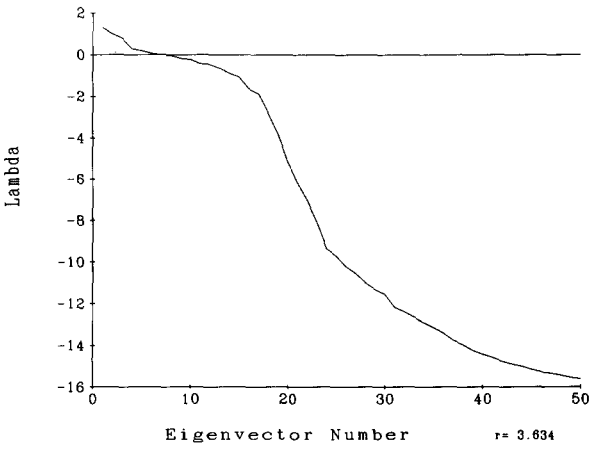

Fig. 7. The spectrum of Lyapunov exponents, with $r = 3.634$, $a = 18\frac{2}{3}$ and $N = 50$. There are six positive Lypunov exponents. The Lyapunov dimension is roughly 11.1.

7. Description of space–time intermittency

Our primary interest in this paper is the complicated space–time intermittency observed in Region I. For convenience, we pick our initial conditions to be symmetric, with two spatial domains, since this is the simplest case with the correct qualitative behavior, and consider $a \approx 20$. We should emphasize, however, that except for a few details, most of our remarks apply equally well to a wide range of parameter values and initial conditions.

Space–time intermittency is illustrated in fig. 1. As seen in fig. 1(c), the distinction between chaotic and laminar behavior is sharp. Chaos is confined by the domain walls, so that it exists throughout one domain, but almost not at all in the other. This comes about because the coupling between internal degrees of freedom inside a given domain is quite strong, whereas coupling between points in neighboring domains much weaker. Disturbances have a difficult time propagating across the domain walls. This can be seen eq. (8): Near a nodal point, $x'' \approx 0$, and also $x_{t+1} \approx x_t$. Thus information propagation through a node depends on higher order terms, which are typically small. This has been studied numerically by Kaneko [5].

Up until now we have been somewhat vague about what we mean by "laminar". Plotting the temporal behavior at a fixed lattice point makes this clear, as shown in fig. 1(d): A given point is *laminar* when its motion is nearly periodic. "Nearly" is a qualitative distinction, which requires an arbitrary threshold to be well defined. Since the distinction between laminar and chaotic is so sharp, this does not present a problem in practice. As seen in fig. 1(d), the temporal period during laminar bursts is typically approximately 2, 4, 8, or 16. Over one iteration the deviation from periodicity is small, but over many iterations there can be a significant drift in the position of the orbit. During a given laminar burst there can be "bifurcations" in the approximate period, as seen in the fig. 1(d). During the chaotic bursts, in contrast, there is no apparent period.

One immediate question is how many degrees of freedom are involved. To get an idea of this, we computed the spectrum of Lyapunov exponents, as shown in fig. 7, and found six positive Lyapunov exponents, giving a Lyapunov dimension [17] of roughly 11.1. This varies with parameters, but it does make it clear that quite a few modes are participating, and that the space–time intermittency that we are observing is not a transition phenomenon.

An indication of the sharp distinction between laminar and chaotic states can be obtained by linearizing the system at each iteration and plot-

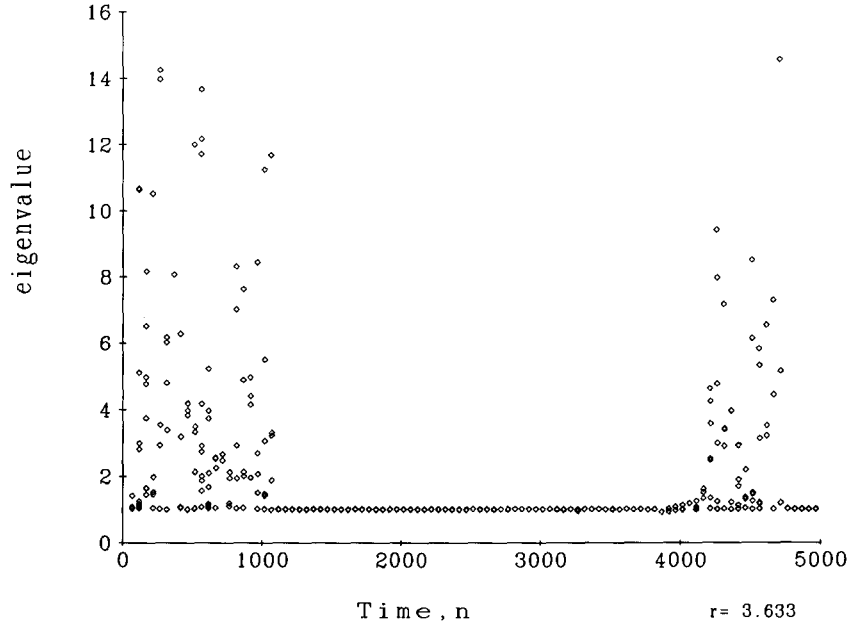

Fig. 8. The eigenvalues of the Jacobian matrix greater than one are plotted as a function of time, illustrating the sharp distinction between the chaotic and laminar phases. Notice that during the laminar bursts there are two eigenvalues greater than one.

ting eigenvalues. Since the laminar states have a typical period of 8, we compose the Jacobian matrix 8 times and compute the largest eigenvalue at different times. The result is shown in fig. 8. During the fully laminar bursts, i.e., when both domains laminar at once, the largest eigenvalue is very close to one. During the chaotic intervals, the largest eigenvalue undergoes large fluctuations, ranging from one to fifteen in a short time.

A frequency histogram of the lengths of the laminar bursts gives an impression of the statistical properties. We label a given lattice site i laminar at time t if $|x_{t-8}(i) - x_t(i)| < \varepsilon$ where $\varepsilon \approx 0.0004$. Otherwise we assume that it is chaotic. The number 8 enters the definition because the period in the laminar regions is typically 8 or less. The resulting histogram is shown in fig. 9. As can be seen from the figure, there is a range in which the histogram decays roughly as a power law, although there is a pronounced peak for laminar bursts of length approximately 1000.

The type of behavior in a given domain is quite fluid. At any given time, the lattice can be entirely chaotic, entirely laminar, or alternatively, as in fig. 1(c), one domain may be chaotic while another is laminar. A feeling for the interaction between the

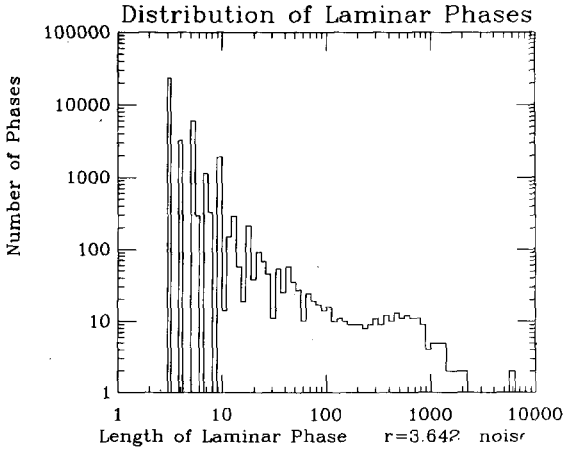

Fig. 9. A frequency histogram of the lengths of the laminar phases.

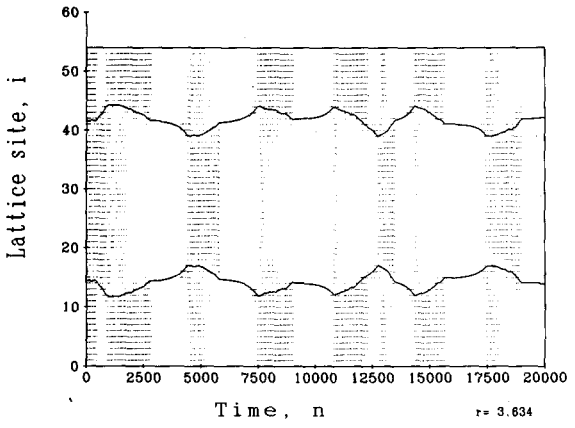

Fig. 10. The time evolution of the chaotic and laminar phases. Chaotic regions are shaded, and laminar regions are left blank. The nodal positions are shown as dark lines.

chaotic and laminar phases can be obtained by plotting them as they evolve in time. Using the definition of laminar behavior given above, in fig. 10 we shade in the chaotic regions of the lattice at sequential times. The nodal points separating the two domains are shown with dark lines. This plot is symmetric due to the symmetry of the initial condition. Note that because of the periodic boundary conditions the sides of the figure should be thought of as connected.

8. Explanation à la Crutchfield

The central question is: What causes the transitions from one type of behavior to another? As a starting hypothesis, we conjecture that this is a type of Crutchfield intermittency, in which the size of a domain acts as a bifurcation parameter controlling the internal dynamics. Since the motion of the domain walls is at least apparently chaotic, this generates intermittent bursts.

To demonstrate that the domain size does indeed act as a bifurcation parameter, we surpress the natural motion of the domain walls by explicitly pinning them with fixed boundary conditions. This allows us to position the nodes at will, creating one domain at a time. We keep the vertical position of the nodes constant at roughly the value they occur at in the unpinned system.

As we vary the domain size in the pinned system, we observe two types of behavior:

1) When the size of the domain is near a half-integral number of natural wavelengths, the motion asymptotically approaches a stable cycle whose spatial oscillations are at the natural wavelength.

2) When the size of the domain is not near a half-integral number of natural wavelengths the asymptotic motion is chaotic.

A typical sequence of lattice configurations obtained by varying the domain size L is shown in fig. 11. For $L = 30$, the lattice settles into a stable cycle whose spatial period is roughly one and a half natural wavelengths. When $L = 35$ the solution is chaotic, but when increased still further so that $L = 40$, it once again settles into a stable periodic state but has now added an extra half oscillation, so that it again has roughly the natural spatial wavelength.

Fig. 12 provides a summary of this behavior. To determine whether the dynamics at a given time is chaotic or periodic, we test for approach to a periodic attractor in the same way that we previously tested for laminarity. At each value of L we plot the number of iterations needed to approach a stable periodic cycle. As seen in fig. 12 there is a steady alternation between chaotic and laminar behavior as L is varied. The system is attracted to a stable cycle whenever the domain size is near a half-integral number of natural wavelengths*.

Fig. 12 clearly shows that the domain size acts as a bifurcation parameter inducing transitions from periodic to laminar behavior. The unpinned system is much like the pinned system, except that the domain walls are not fixed, and consequently there are no stable periodic orbits. As the domain

*It remains unclear whether the apparently chaotic behavior of the pinned system is truly chaotic or just very long lived metastable bursts, as illustrated in fig. 13. For the unpinned system this is irrelevant, since all that is required is that the time scale for metastability is longer than that of the intermittent bursts, which is clearly the case.

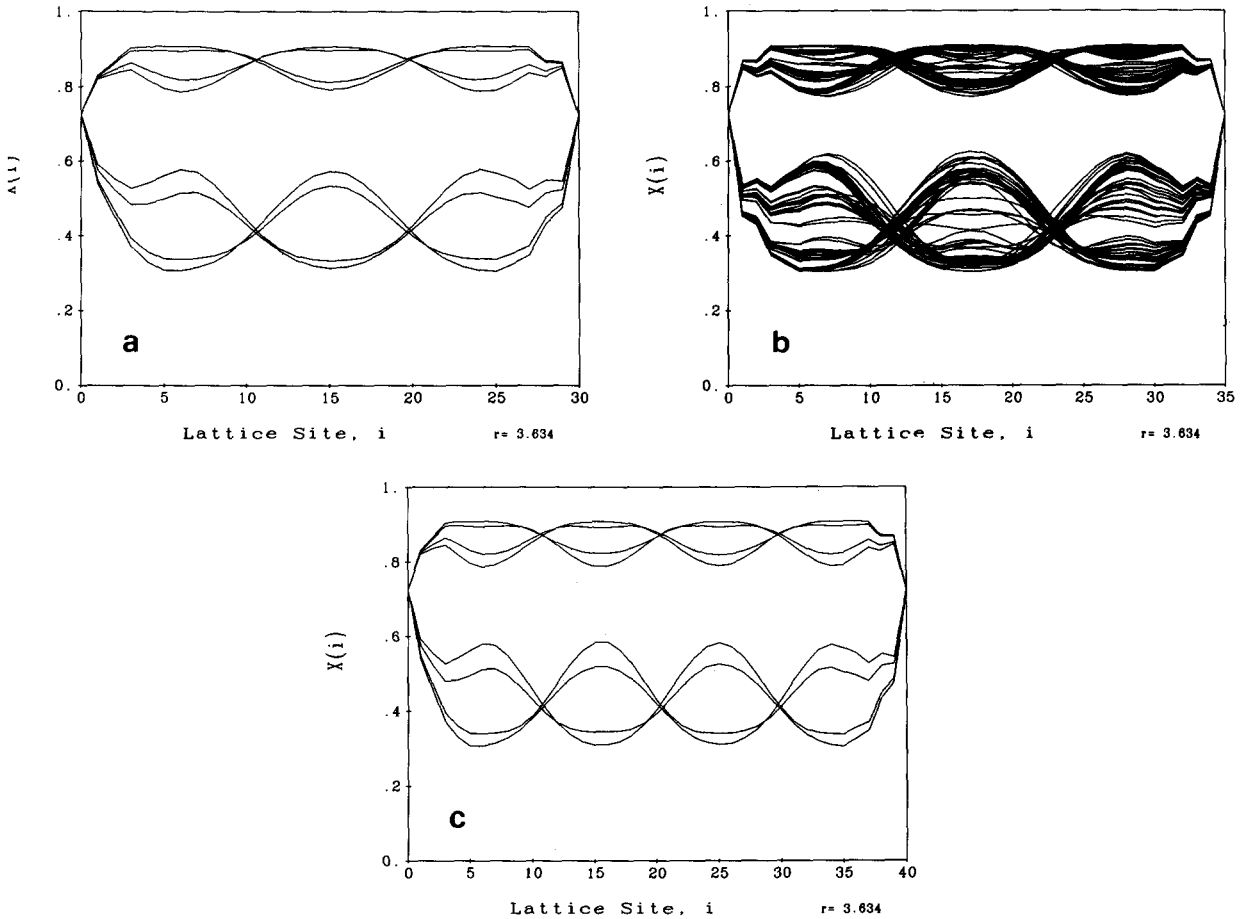

Fig. 11. A sequence of lattice configurations as the aspect ratio is varied at $r = 3.633$, using fixed boundary conditions to pin the domain walls. $A = 2$ throughout. (a) $N = 30$, yielding a stable periodic cycle with a spatial period of one and a half natural wavelengths; (b) $N = 35$, chaotic motion; (c) $N = 40$, a stable periodic cycle with a spatial period of two.

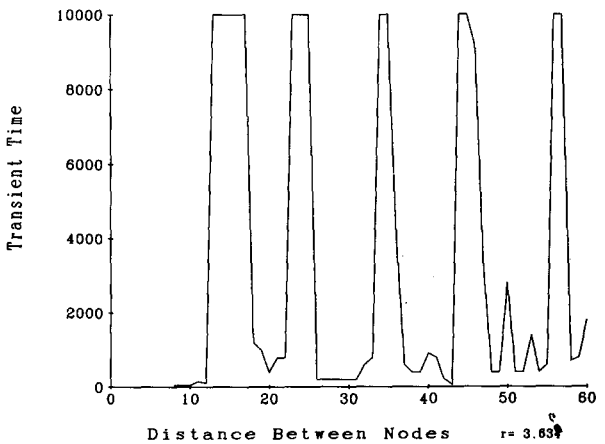

Fig. 12. Number of iterations for approach to stable periodic state as a function of the aspect ratio, using fixed boundary conditions as in fig. 11. Providing the domain size L is roughly a half-integral number of wavelengths of the natural wavelength, the lattice asymptotically approaches a stable periodic cycle; otherwise the solution is chaotic. (There is also metastable chaos; see fig. 13 and the remarks in the text.)

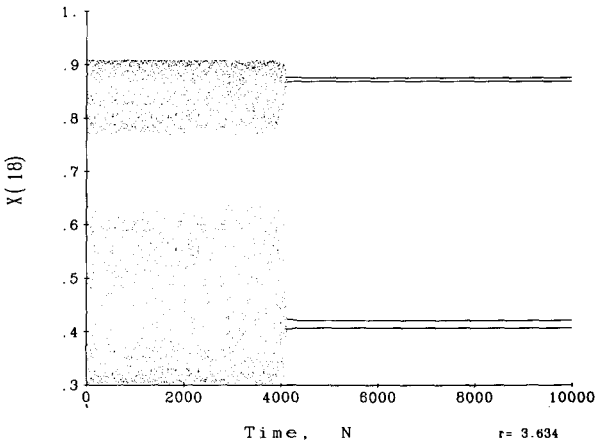

Fig. 13. An illustration of metastable chaos in the pinned system, obtained by plotting the time series at a fixed lattice site. ($A = 2$, $N = 36$, $i = 18$, $r = 3.633$). The solution behaves chaotically until it settles onto a stable cycle, after roughly 4,000 iterations.

walls move they induce spatially localized bifurcations from chaotic to nearly periodic behavior. The slow time scale of the domain wall motion makes these bursts quite long. The transients tend to favor chaos, since the domain size must remain in the periodic range long enough for the chaotic transients to die down.

9. Explanation à la Pomeau–Manneville

A question that immediately comes to mind is the nature of the connection between the laminar states of the unpinned system and the stable periodic states of the pinned system. Are the laminar states associated with unstable periodic cycles? To test this, we used a modified Newton's method to search for unstable periodic cycles in the unpinned system. When we gave our Newton's method arbitrary initial conditions, we found a plethora of diverse unstable periodic cycles. To restrict ourselves to the relevant solutions, we picked our initial conditions for the Newton's method by stopping the system at the beginning of a laminar burst. Typical solutions obtained in this manner are shown in fig. 14. Their spatial and temporal properties are similar to those of the corresponding laminar phases. Furthermore, the largest eigenvalue of these cycles is always slightly greater than one, e.g. 1.001. Each laminar burst can be associated with a nearly stable cycle whose properties are very close to those of the burst.

This suggests an alternate explanation for intermittency more along the lines of the Pomeau–Manneville theory: The chaotic attractors underlying the behavior of this system contain nearly stable cycles. In the course of chaotic motion on its attractor, from time to time the system finds itself near one of the nearly stable cycles. The close proximity of the eigenvalue to one means that once near the cycle the orbit stays near it for some time, causing long bursts of laminar behavior.

To demonstrate the validity of this view, we study the divergence during a laminar burst. Using our Newton's method we find the nearly stable cycle associated with a given laminar burst and take the difference from the lattice configuration during the burst. We plot the Euclidean norm of this difference as a function of time, as shown in fig. 15. As expected the divergence is nearly exponential during the laminar burst.

The important difference from Pomeau–Manneville intermittency is that the near stability of the underlying cycles persists through a wide range of parameters. The persistence of the near stability property of the unstable cycles can be understood in terms of their relation to the stable attractors of the pinned system. For example, compare fig. 12 to fig. 14. The lattice configuration of the unpinned cycle is nearly identical to that of the pinned system; similar comparisons can be made for other fixed points. This clearly demonstrates that there is a one-to-one correspondence between the stable cycles of the pinned system and the nearly stable cycles of the laminar system. The important difference is that the unpinned domains have additional eigenvalue whose moduli are slightly greater than one. These eigenvalues correspond to the possibility for nodal motion, and the proximity to one corresponds to

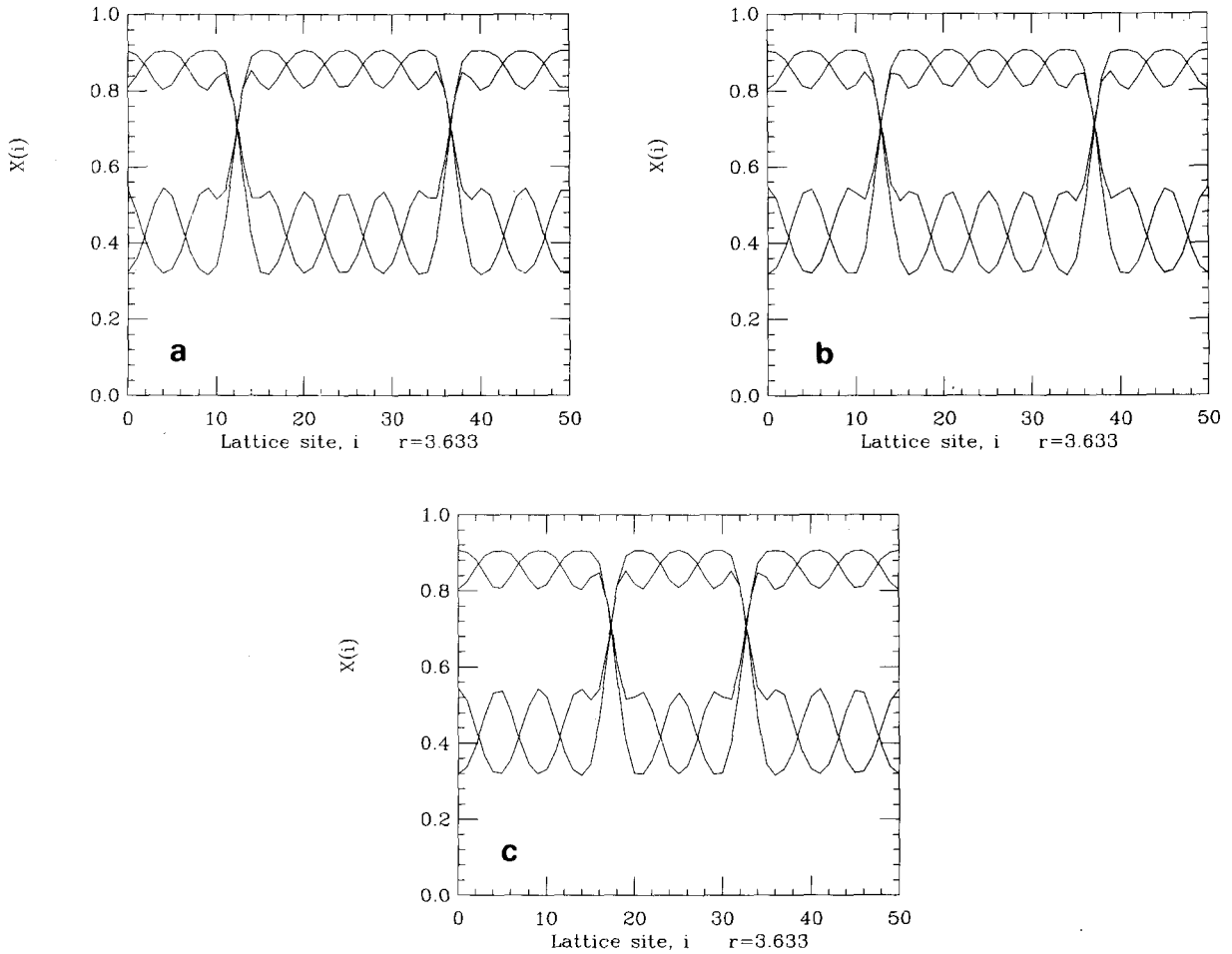

Fig. 14. A few examples of the nearly stable cycles underlying the laminar bursts. (a) A $\{5,5\}$ cycle, i.e., a two domain cycle with five half-integral multiples of the natural wavelength in each domain. (b) A comparison to a typical lattice configuration during the corresponding $\{5,5\}$ laminar burst. (c) A $\{7,3\}$ cycle. The largest eigenvalues are (a) 1.0019; (c) 1.0011. Note the correspondence to the stable cycles shown in fig. 11, which have roughly the same parameter values.

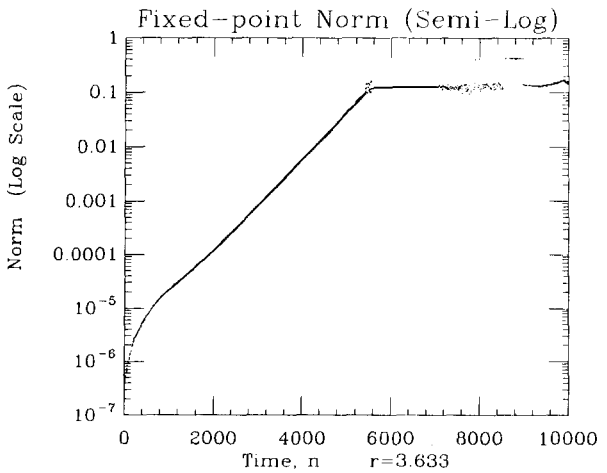

Fig. 15. Divergence during a laminar burst. The unstable cycle associated with a laminar burst is subtracted from the lattice configuration of the burst, and the Euclidean norm is plotted as a function of time on a semi-log scale. This clearly indicates the exponential divergence from the unstable cycle.

the long time scale of the motion. Since the stable cycles of the pinned system are stable throughout a wide range of parameter values, it is to be expected that the slight destabilization caused by unpinning them persists throughout roughly the same parameter range. This explains why the intermittency that we observe is robust while the Pomeau–Manneville type is not.

At a given set of parameter values there are many nearly stable cycles. They share the property that the spatial oscillations inside of each domain have roughly the natural wavelength, but differ in the total number of oscillations in each domain. Suppose, for example, that the system has two domains and that parameters are picked so the total lattice size is roughly 5 natural wavelengths. There are then five* nearly stable cycles, which can be labeled $\{1,9\}$, $\{2,8\},\ldots,\{5,5\}$, according to the number of half-integer multiples of the natural wavelength in each domain. As an example a $\{5,5\}$ and a $\{3,7\}$ cycle are shown in fig. 14.

This classifies the fully laminar states, i.e., the states in which all the domains are laminar at the same time. As we have seen, however, one domain can be laminar while the others are chaotic. This can be explained by the fact that, except for the coupling through the motion of the domain walls, different domains behave largely independently of each other. As a result the phase space can roughly be divided into hyperplanes, one for each domain. Each hyperplane contains the projection of the nearly periodic states, one for each commensurate number of natural wavelengths. If the system arrives near one of these points, a laminar burst results. Each hyperplane is more or less independent, except for the motion of their mutual domain walls. In general, we hypothesize that the number of eigenvalues greater than one is equal to the number of domain walls.

10. Motion of domain walls

The results we have presented suggest that the space–time intermittency of this type can be understood in terms of a reduced slow scale dynamical system describing the nodal motion, along the lines of eq. 1b. Such a system would presumably include two types of variables, some in terms of statistical properties of the internal degrees of freedom in the domains, the others giving the positions of the nodes. Unfortunately, we have not been able to accomplish this. Even without such an explicit description, however, several properties of the motion can be immediately deduced.

A careful study of fig. 10 reveals that the motion of the domain walls is qualitatively different, according to the nature of the two domains on either side of the wall. There are three cases:

1) *Both domains chaotic*: The nodes appear to make a random walk.

2) *One domain chaotic while the other is laminar*: The chaotic domain steadily encroaches upon the laminar domain.

3) *Both domains laminar*: There is a smooth invasion of one domain by the other, which becomes increasingly rapid as it proceeds.

Case 1, in which both domains are chaotic, is perhaps the most straightforward: The chaotic motion inside each domain causes an effectively random vibration of the node; when two systems are coupled together the resulting movement of the node follows a random walk. This continues until one of the domain sizes becomes commensurate with the natural wavelength long enough for chaotic transients to decay, and the domain becomes laminar.

Case 2, in which one domain is chaotic while the other is laminar, is more complicated. A partial explanation is that the lowest wavelengths are the most unstable in chaotic domains, as demonstrated in fig. 16. The most unstable modes are associated with the largest Lyapunov numbers. Just as in linear problems there is an eigenvector associated with each eigenvalue, in nonlinear problems there is a Lyapunov vector associated with each Lyapunov number. For a chaotic system the Lyapunov vectors vary chaotically in time, just as the solution does. Nonetheless, the Lyapunov vectors can have well defined statistical properties.

*Because of symmetry $\{1,9\} = \{9,1\}$, $\{1,8\} = \{8,1\}$, etc.

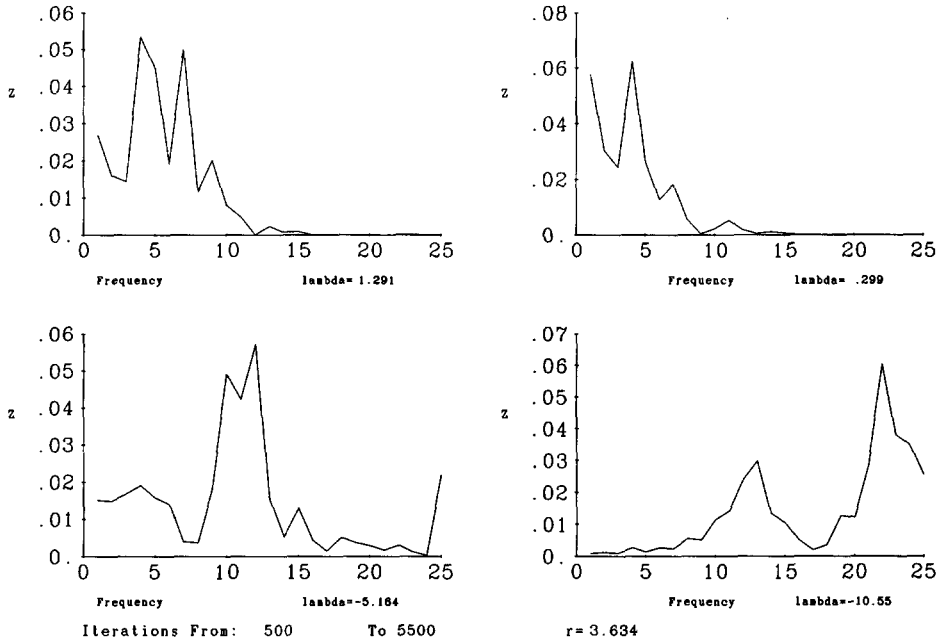

Fig. 16. The frequency spectrum of four typical Lyapunov vectors. At parameter values where the behavior is chaotic, the Lyapunov vectors (which are themselves chaotic) are sampled at different time steps. For each sample we take the square of the Fourier transform of the lattice configuration. The squares of the Fourier transforms are averaged together to produce a spatial power spectrum. This gives an indication of the spatial frequencies associated with each Lyapunov mode. Four different examples are given, with typical examples of a Lyapunov vector and the corresponding spectral average. The Lyapunov exponents are ordered according to their size, and the subscript indicates this ordering. (a) $\lambda_1 = 1.291$; (b) $\lambda_3 = 0.299$; (c) $\lambda_{20} = -5.164$; (d) $\lambda_{27} = -10.55$.

By averaging the square of the Fourier transform at each iteration to obtain the spatial power spectrum we get a good idea of the spatial wavelengths associated with each Lyapunov vector. Four typical cases are shown in fig. 16. For both of the vectors associated with unstable modes the spectra show strong low frequency components, even though the actual peak occurs near the natural spatial frequency. The Lyapunov vectors associated with the stable modes, in contrast, are peaked at higher frequencies and have less low frequency components. Thus higher frequencies are damped while lower frequencies grow. The instability of the chaotic state is much greater than that of the laminar state, so in the competition the size of the chaotic domains grows at the expense of the laminar domains.

Case 3 is probably the best understood: When both domains are laminar, as we demonstrated in fig. 15, there is a smooth exponential escape from the nearly stable cycle. Since the motion of the domain wall is precisely the mode associated with this eigenvalue, the position of the wall exponentially moves away from its value at the beginning of the burst. Which direction it moves is influenced by the position of the point in phase space upon rejection. Typically the phase space point diverges faster in one projection than it does in the other, causing a net motion of the domain wall.

An interesting property of this type of intermittency is the remarkable insensitivity to external noise. We experimented by adding random fluctuations throughout the lattice, at noise levels ranging from 10^{-7} to 10^{-2}. We observe no perceptible change in the distribution of the length of the laminar regions until the noise level reaches 10^{-3}, except for truncation in the length of the

longest laminar bursts. This is hard to measure because of the weak dependence on the noise level, and the difficulty of gathering statistics*. The general insensitivity to noise is presumably a consequence of the fact that domain wall motion is largely unaffected by external noise.

11. N $1/f$ noise

There are many natural phenomena whose power spectra scale asymptotically at low frequencies like $1/f$. There are many theories for this [18], and it seems likely that $1/f$ noise is not a single phenomenon but a family of phenomena that may have diverse explanations. One such explanation is Pomeau–Manneville intermittency, which generically generates a $1/f$ spectrum [19,20]. The applications are severely limited, however, since Pomeau–Manneville intermittency is a transition phenomenon. In contrast, in many physical settings $1/f$ noise occurs through a very broad range of parameters. Our model potentially solves this problem. Since the laminar bursts are governed by nearly stable cycles, the spectral properties are like those of Pomeau–Manneville, but unlike Pomeau–Manneville, our model is robust.

An interesting aspect of the spectral behavior is that the properties of spatial averages are significantly different from those at a single point. This comes about because of the intrinsic difference between the fully laminar phases and the mixed chaotic/laminar phases (case 3 vs. case 2 above). When the lattice is fully laminar, the invasion of one domain by another is exponential, with an arbitrarily long persistence time†. For the mixed chaotic–laminar cases, in contrast, the chaotic domain invades the laminar domain in a fairly steady way, putting an upper limit on the persistence of a laminar burst.

If a time series is obtained by sampling at a single point on the lattice, the laminar bursts are a mixture of fully laminar and mixed cases. The resulting power spectrum is somewhat complicated, as shown in fig. 17(a). There is some evidence of low frequency power law scaling of

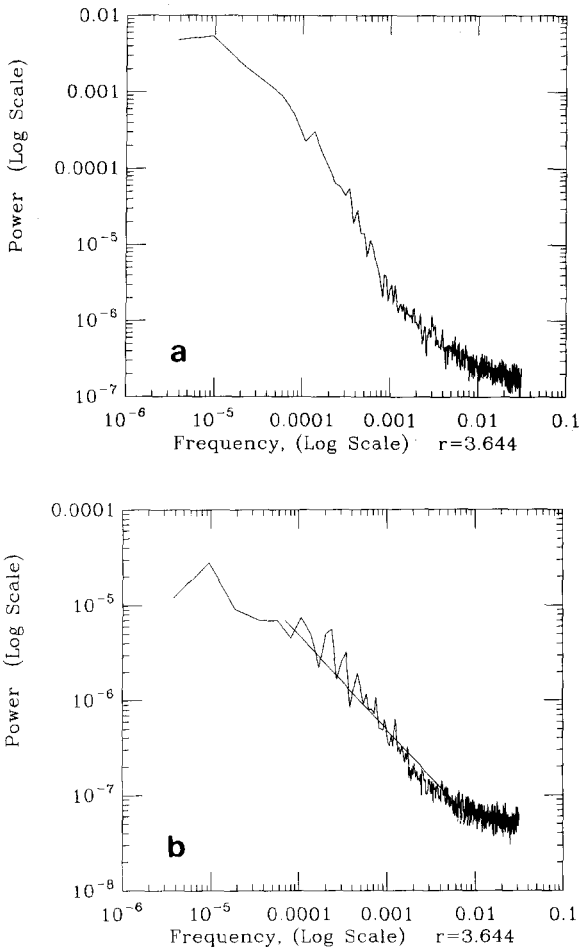

Fig. 17. (a) A temporal power spectrum, obtained by sampling a single lattice point ever 8th iteration and computing a 65,536 point Fourier transform and frequency averaging. The scaling at low frequencies behaves roughly as $f^{-\alpha}$. At this parameter value $\alpha \approx \frac{5}{2}$, but this varies with r. (b) A temporal spectrum obtained by taking the Euclidean norm of the difference between the lattice configuration and that 8 timesteps later, and Fourier transforming the result. As can be seen by comparing with the line, the low frequency behavior is roughly $1/f$.

*An estimate of this effect can be made by assuming exponential divergence from the unstable cycle. Assuming that a laminar burst persists until the divergence from the cycle is of order one, the persistence time τ is roughly $\tau = \log 1/\sigma\Lambda$, where σ is the noise level and $\Lambda = \log \lambda$, where λ is the largest eigenvalue. At floating point precision, for example, we expect the longest burst to persist for about 20,000 iterations.

†Except for the truncation due to external noise, as discussed earlier.

the form $f^{-\alpha}$, but the value of α depends on r. For the case shown $\alpha \approx \frac{5}{2}$.

When a time series is obtained by a bulk measurement, in contrast, the low frequency divergence of the power spectrum is roughly $1/f$, as shown in fig. 17(b). By "bulk measurement", we mean any property that is an average property of the whole system, as opposed to a single point. For example, we took the norm of the difference of two lattice configurations separated by eight time steps (to get rid of the intrinsic periodicity of the laminar bursts). Doing this at successive times gives us a time series, whose power spectrum is shown in fig. 17(b). This spectrum has a fairly pronounced $1/f$ divergence over two decades. The reason for the difference between figs. 17(a) and 17(b) is clear: The bulk measurement suppresses the mixed laminar bursts. Although the analyses of refs. [20] and [21] were made with Pomeau–Manneville intermittency in mind, it is clear that their arguments also apply to the fully laminar bursts in our case, since the only necessary property is that the laminar bursts be dominated by approach to an unstable cycle. Thus, we expect that the $1/f$ low frequency behavior of the spectrum is a generic property of the type of intermittency that we discuss here, providing the spectrum is based on a bulk measurement.

12. Connection to experiments

Our model can be taken on two different levels of generality. What we have described here includes several aspects, such as kink conservation caused by semiperiodic behavior or the extence of a reverse period doubling sequence. These features might well be observable in experiments, but we would like instead to stress the more general aspects of this behavior, which probably have a much wider range of applicability.

Perhaps the two most essential aspects are the existence of spatial domains with mobile domain walls, and the possibility for spatially localized bifurcations between two different types of behavior as the domain size varies. In the example we studied here the bifurcations are associated with the natural spatial frequency of the internal oscillation, but in general the bifurcations might result from other effects. The $1/f$ low frequency behavior of the bulk spectrum should be present as long as there is a laminar phase with nearly periodic behavior. Another general feature is the persistence of the behavior through a range of parameter values, rather than just near a bifurcation point.

At this point we have no definitive experimental test for this type of intermittency, except to suggest searching for the characteristics listed above. Because this phenomenon is generic rather than transitional, there are not likely to be universal scaling laws under variation of parameters, such as for Pomeau–Manneville intermittency.

Perhaps the most likely physical application is to solid state devices, which have spatial domains and robust $1/f$ noise over wide parameters ranges. For experimental verification, any technique which allows spatial visualization of the behavior would help make this connection firmer; it should also be possible to investigate the relevant theoretical models to see whether or not there is any correspondence. Spectra in these cases usually involve bulk measurements; our model suggests that more localized measurements might produce different spectral behavior.

Reaction–diffusion systems provide another natural place to search for experimental applications. In fact, one of the most prominent $1/f$ noise theories is based on reaction–diffusion [18]. A likely application is presented by the Kuramoto–Shivashinky equation, which is known to have space–time intermittency, and as far as we know has not been investigated in any detail [22]. Video feedback provides a convenient way to simulate reaction–diffusion phenomena; space–time intermittency is observed there, which may well be of this same type [23].

There are many other physical phenomena that display space–time intermittency, including doubly rotating Taylor–Couette flow [1], plasma

pinches [24], Raleigh–Bénard convection [25], and the Eckhaus instability [26]. At this point we have no idea whether any of these phenomena are related to the behavior that we have discussed here. We hope that others will investigate these and other instances of space–time intermittency, to explore the possibility of such a relationship.

We by no means intend to suggest that this is the only possible model for space–time intermittency. As already mentioned, either Pomeau–Manneville or crisis intermittency can manifest themselves in space as well as time, although with properties that are substantially different from what we have described. We expect that there are also new varieties of space–time intermittency, as yet unexplained.

13. Conclusions

There are a few key properties that provide clues to expect the type of space–time intermittency that we have described here:

1) Well defined spatial domains.

2) A bifurcation between two different types of behavior which can be induced by changing the domain size.

3)Slow time scale chaotic motion of the domain walls.

In the system we studied here the bifurcations are naturally understood in terms of the natural frequency; if the size of the domain is pinned at close to a half-integral multiple of the natural wavelength, there is a periodic attractor; if this condition is not met it is chaotic. When the domains are allowed to move the periodic attractors are destabilized, but only just barely; the size of the domains changes slowly compared to the internal motion, creating long lived "laminar" phases that are approximately periodic. This behavior has elements of Crutchfield intermittency, but also elements of Pomeau–Manneville intermittency. In contrast to Pomeau–Manneville, this typically exists through a broad range of parameters.

Perhaps the principal problem remaining for further investigation is an explicit representation of the slow scale motion in terms of a low dimensional dynamical system. This might be stated, for example, in terms of the nodal positions and a few statistical properties of the system. There may well be closure problems, etc., but even an approximate scheme would be very nice.

In conclusion, we have analyzed a variety of space–time intermittency observed in lattice maps, which is robust under changes in parameters. Although the number of different systems in which the behavior is the same in a detailed way is probably small, the broad outlines, i.e., spatially localized bifurcations caused by the modulation of domain size, are likely to occur in many different systems. We hope that our work stimulates further investigation of this fascinating phenomenon.

Acknowledgements

We would like to thank Jim Crutchfield, Kunihiko Kaneko, Gottfried Mayer-Kress, Norman Packard, and Yves Pomeau for helpful comments. One of us (JDK) would like to thank the staff of the CNLS for their hospitality during his visit, and Henry D. I. Abarbanel and the UCSD Institute for Nonlinear Science for making this possible. This work was partially supported by the U.S. Air Force Office of Scientific Research under Grant No. ISSA-86-00017.

Note added in proof

At time of printing, we became aware of the work of S.P. Kuznetsov and A.S. Pikovsky, Physica 19D (1986) 384. This work shows that the system discussed in this paper has universal properties.

References

[1] C.D. Andereck, S.S. Liu and H.L. Swinney, J. Fluid Mech. 164 (1986) 155–183.

[2] J.P. Crutchfield, Noisy Chaos, U.C. Santa Cruz Ph.D. Thesis (1983).
[3] R.J. Deissler, Physics Letters A100 (1984) 451.
[4] K. Kaneko, Prog. Theo. Phys. 72 (1984) 480.
[5] K. Kaneko, Prog. Theo. Phys. 74 (1985) 1033, and Physica 23D (1986) 436.
[6] I.P. Waller and R. Kapral, Phys. Rev. A30 (1984) 2047.
[7] N. Metropolis, M.L. Stein and P.R. Stein, J. Combin. Theory, Ser. A 15 (1973) 25–44.
[8] M. Feigenbaum, J. Stat. Phys. 19 (1978) 25–52.
[9] J.D. Keeler, "An explicit relation between coupled maps, cellular automata, and reaction–diffusion equations", UCSD preprint.
[10] Y. Pomeau and P. Manneville Comm. Math. Phys. 74 (1980) 189.
[11] C. Grebogi, E. Ott and J. Yorke, Physica 7D (1983) 181.
[12] J.P. Crutchfield, "Stability and Prediction in Classical Mechanics", UCSC senior thesis (1979).
[13] E.A. Celier and R. Kapral, "The global structure of basins of attraction: A study of Rossler's equations", preprint.
[14] E.N. Lorenz, Ann. N.Y. Acad. Sci. 357 (1980) 282.
[15] J. Crutchfield, J.D. Farmer, N. Packard, R. Shaw, G. Jones and R.J. Donnelly, Physics Letters A76 (1980) 1.
[16] J. Crutchfield and K. Kaneko, as yet unpublished.
[17] J. Kaplan and J.A. Yorke, Functional Differential Equations and Approximation of Fixed Points, H.O. Peitgen and H.O. Walther, eds. (Springer, New York, 1979).
[18] P. Dutta and P.M. Horn, Rev. Mod. Phys. 53 (1981) 497.
[19] P. Manneville, Journal de Physique 41 (1980) 1235.
[20] A. Ben-Mizrachi, I. Procaccia, N. Rosenberg, A. Schmidt and H.G. Schuster, Phys. Rev. A 29 (1984) 975.
[21] T. Geisel and S. Thomae, Phys. Rev. Lett. 52 (1984) 1936.
[22] Basil Nicols and Stephan Zalesky, private communications.
[23] J. Crutchfield, "Space–time dynamics of video feedback", video tape.
[24] R.G. Watt and R.A. Nobel, Phys. Fluids 26 (1983) 1168.
[25] G. Ahlers and R.W. Walden, Phys. Rev. Lett. 44 (1980) 445.
[26] G.Ahlers, Lecture notes, University of California Summer School in Nonlinear Science, (UCSD, La Jolla CA, August 1985).